Supplement of Atmos. Chem. Phys., 25, 16713–16727, 2025
https://doi.org/10.5194/acp-25-16713-2025-supplement

Atmospheric Chemistry and Physics Open Access

Supplement of

Criegee + HONO reaction: a bimolecular sink of Criegee, and the missing non-photolytic source of OH•

Vishva Jeet Anand et al.

Correspondence to: Pradeep Kumar (pradeep.chy@mnit.ac.in)

S1 Geometries and frequencies

Table S1: Cartesian coordinates and all normal mode frequencies of the optimized geometries calculated at M06-2X/aug-cc-pVTZ level of theory.

Species	Cartesian coordinates (Å)				Frequency (cm^{-1})		
	C	1.057098	-0.186174	0	538.15	697.71	927.20
	H	1.006167	-1.269154	0	1023.97	1260.68	1433.37
CH_2OO	H	1.966689	0.398409	0	1630.89	3139.98	3290.59
	O	0	0.459688	0			
	O	-1.16443	-0.211215	0			
	N	0	0.507841	0	578.24	700.42	905.04
	O	0.882551	-0.567177	0	1342.39	1841.11	3830.83
HONO	O	-1.101711	0.141484	0			
	H	1.753278	-0.149345	0			
	O	1.498972	-1.038397	0.244942	65.11	92.16	142.24
	O	1.726641	0.149063	-0.424616	166.18	224.27	273.11
	C	1.420998	1.180384	0.176904	525.70	695.30	769.68
	H	1.576962	2.106616	-0.363492	876.31	1010.42	1052.16
RC1	H	1.036523	1.112197	1.187687	1107.39	1256.42	1448.64
	N	-1.27518	0.258091	0.073874	1557.40	1679.05	1793.75
	O	-1.091011	-1.060536	-0.093095	2990.53	3141.61	3286.10
	H	-0.100636	-1.185364	0.034644			
	O	-2.398675	0.584571	-0.031904			
	O	1.650665	-0.899517	0.185806	-248.25	103.69	196.24
	O	1.542624	0.364395	-0.446018	243.30	340.61	400.60
	C	0.909591	1.185914	0.23834	522.64	776.50	782.50
	H	0.706837	2.142819	-0.228811	880.96	1088.56	1139.31

TS1	H	0.750931	0.992577	1.29178	1183.44	1244.33	1437.18
	N	-1.137944	0.151896	0.035635	1635.17	1684.49	1795.32
	O	-0.807104	-1.120664	-0.039819	1974.20	3146.01	3282.87
	H	0.257887	-1.162149	0.072964			
	O	-2.287134	0.386785	-0.051896			
PC1	O	-1.891229	0.38775	0.49254	76.22	188.29	332.59
	O	-1.329506	-0.452034	-0.504135	421.52	455.14	553.61
	C	-0.157737	-0.957206	-0.020654	605.00	738.56	930.50
	H	0.182808	-1.741835	-0.690912	972.37	1116.88	1203.36
	H	-0.218591	-1.294705	1.012421	1297.85	1374.49	1439.18
	N	0.95063	0.094534	-0.02322	1452.24	1502.00	1713.12
	O	0.652686	1.231141	-0.303473	3113.19	3190.86	3755.70
	H	-1.488438	1.239765	0.262016			
	O	2.045078	-0.307073	0.277935			
OH	O	0	0	0.107992	3769.62		
	H	0	0	-0.863937			
NO_2	N	0	0	0.314473	783.52	1465.18	1755.31
	O	0	1.090255	-0.137582			
	O	0	-1.090255	-0.137582			
HCHO	O	-0.670517	0.0000227	-0.000001	1213.53	1273.49	1539.85
	C	0.525515	0	0.000003	1869.05	2945.55	3015.83
	H	1.105357	-0.938452	-0.000006			
	H	1.105686	0.93828	-0.000006			
	C	0.371062	0.018585	0.00005	161.4785	208.2494	291.0197
	O	-0.558411	-0.81759	-0.000008	329.946	366.3571	493.4939
	O	-1.838845	-0.328935	-0.000003	609.8208	827.3278	925.0805
	C	0.053885	1.456083	-0.000006	953.0914	989.3886	1085.6587

	H	-0.57815	1.668238	0.865389	1102.011	1316.0578	1393.969
$(CH_3)_2COO$	H	0.954341	2.062465	-0.000046	1411.6898	1442.1269	1466.9645
	H	-0.578203	1.668145	-0.86537	1474.3344	1486.7659	1654.0743
	C	1.752599	-0.524309	0.000001	3059.282	3065.4337	3109.8178
	H	2.288094	-0.158843	0.877727	3121.9032	3182.2265	3183.8812
	H	1.739149	-1.610169	0.000607			
	H	2.287541	-0.159787	-0.878484			
	O	-0.323346	1.788465	-0.127155	40.9916	65.3092	94.8686
	O	-0.933456	0.707341	-0.762464	143.887	165.0795	182.4321
	C	-1.427404	-0.163929	-0.015067	184.8149	254.8398	336.26
	N	1.668747	-0.491904	0.103393	357.8193	376.4962	494.4218
	O	2.027385	0.75438	-0.212701	601.2322	778.1414	824.8282
	H	1.149904	1.272513	-0.192924	905.477	949.7473	992.8326
	O	2.5751	-1.24643	0.120319	1062.3121	1084.8706	1100.4914
RC2	C	-2.010313	-1.34373	-0.692483	1107.6633	1317.6543	1381.0831
	H	-1.444347	-2.223239	-0.376851	1406.8156	1448.8553	1461.7488
	H	-3.040077	-1.483491	-0.362789	1471.93	1488.8255	1579.3946
	H	-1.962298	-1.240373	-1.771878	1668.5843	1779.7402	2780.974
	C	-1.402643	-0.006457	1.447276	3065.3064	3070.7206	3128.6412
	H	-0.3575	0.00306	1.763655	3129.2175	3189.9646	3191.0969
	H	-1.801638	0.976862	1.69949			
	H	-1.948582	-0.807358	1.935197			
	O	0.550552	-1.91232	-0.157936	-875.0178	88.1328	110.2442
	O	1.027394	-0.718099	-0.761686	141.1228	161.9634	176.0151
	C	1.025985	0.293662	0.000171	241.0089	299.2742	320.3139
	N	-1.317937	0.33477	-0.010799	370.0784	395.3556	489.6676
	O	-1.645557	-0.916254	-0.068479	558.7228	604.2866	812.5142

	H	-0.607076	-1.53411	-0.103381	895.2549	933.636	968.2391
TS2	O	-2.206625	1.124555	0.016787	990.135	1094.7045	1099.1694
	C	1.032531	0.192244	1.478444	1245.2764	1289.6521	1326.3627
	H	2.072829	-0.000888	1.762063	1404.0109	1419.8947	1454.66
	H	0.720659	1.139428	1.908866	1457.975	1469.165	1490.2106
	H	0.422449	-0.627005	1.835792	1618.1624	1686.0865	1860.5208
	C	1.35894	1.574774	-0.666744	3054.66	3071.2572	3137.5137
	H	0.578987	2.294941	-0.418211	3156.4911	3191.39	3222.9338
	H	2.30335	1.947896	-0.267396			
	H	1.423516	1.449212	-1.742853			
	O	1.985793	-0.726895	0.25413	52.4597	162.8702	213.6543
	O	1.28194	0.118675	-0.639404	234.9484	262.3477	282.2477
	C	0.100634	0.559106	-0.067175	326.5011	355.8608	396.5205
	N	-0.876611	-0.653207	0.010107	462.1167	477.6842	583.8607
	O	-0.484791	-1.727573	-0.385388	617.808	757.3543	860.24
	H	1.618317	-1.589659	0.007351	893.1847	962.7302	982.8632
	O	-1.970236	-0.431354	0.465927	1032.5788	1070.5757	1186.0233
PC2	C	0.242791	1.111547	1.33574	1277.0505	1305.6178	1405.298
	H	0.963065	1.92676	1.298642	1412.3545	1436.5532	1478.2497
	H	-0.716779	1.486469	1.679701	1484.8552	1486.8893	1499.1822
	H	0.606302	0.351478	2.020882	1513.7957	1692.8757	3087.5924
	C	-0.498782	1.533219	-1.060518	3094.1386	3167.6738	3174.1824
	H	0.143496	2.409662	-1.110279	3184.9593	3190.5432	3760.4604
	H	-0.555824	1.076113	-2.046571			
	H	-1.491803	1.82556	-0.730883			
$(CH_3)_2CO$	O	0.021464	1.382277	0.000011	111.9307	175.4067	384.5896
	C	-0.005455	0.177931	-0.000082	497.2894	531.5722	796.9533

	C	1.277228	-0.627419	-0.000037	883.6212	934.5994	1075.7547
	H	1.100747	-1.700338	-0.00297	1116.1008	1245.1935	1382.726
	H	1.862521	-0.350951	-0.876226	1390.7895	1465.3831	1477.3376
	H	1.859411	-0.355511	0.87968	1482.7335	1483.9292	1847.1097
	C	-1.300425	-0.59294	-0.000001	3061.2825	3075.9873	3122.6717
	H	-1.338462	-1.24216	-0.876626	3149.0436	3166.3195	3181.8401
	H	-1.338009	-1.242613	0.876335			
	H	-2.146009	0.087933	0.000439			

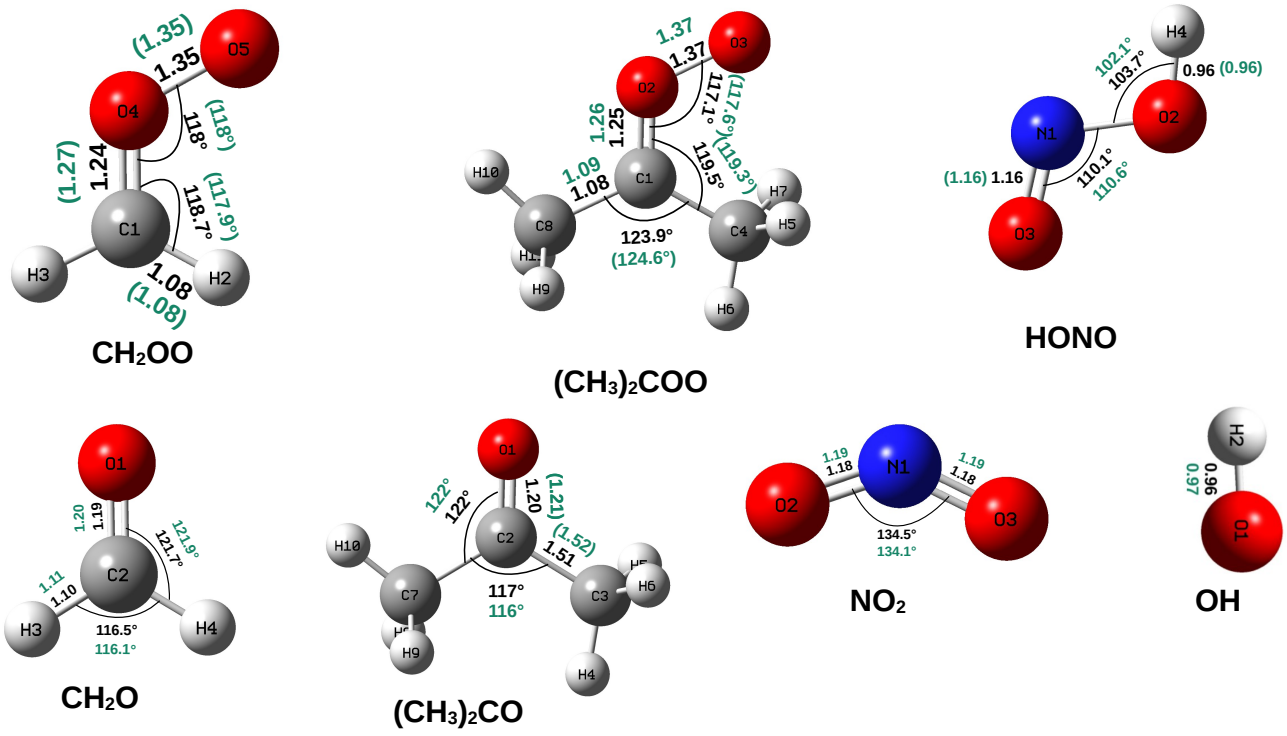

Figure S1: Comparison of geometrical parameters of the isolated species, obtained at M06-2X/aug-cc-pVTZ level of theory (values in bold black) with the available experimental data (values in bold green).[1]

Table S2: Comparison of frequencies (in cm^{-1}) of the isolated species, obtained at M06-2X/aug-cc-pVTZ level of theory with the available experimental data.

Species	Experimental				(M06-2X/aug-cc-pVTZ)			
CH_2OO	848				538.15	1023.97	1630.89	
	908				697.71	1260.68	3139.98	
	1241				927.20	1433.37	3290.59	
	1286							
	1435							
HONO	543	1263			578.24	1342.39		
	596	1700			700.42	1841.11		
	790	3591			905.04	3830.83		
OH	3738				3769.62			
NO_2	750				783.52			
	1318				1465.18			
	1666				1755.31			
HCHO	1167	1249			1213.53	1869.05		
	1500	1746			1273.49	2945.55		
	2782	2843			1539.85	3015.83		
$(CH_3)_2COO$	77	877	1364	2937	111.9307	175.4067	384.5896	497.2894
	125	891	1410	2937	531.5722	796.9533	883.6212	934.5994
	385	1066	1426	2963	1075.7547	1116.1008	1245.1935	1382.7261
	484	1091	1435	2972	1390.7895	1465.3831	1477.3376	1482.7335
	530	1216	1454	3019	1483.9292	1847.1097	3061.2825	3075.9873
	777	1364	1731	3019	3122.6717	3149.0436	3166.3195	3181.8401

Table S3: Frequencies of scan points for CH_2OO + HONO reaction (RC1 to isolated reactants) at M06-2X/aug-cc-pVTZ level of theory. Energies at CCSD(T)/CBS//M06-2X/aug-cc-pVTZ level of theory.

Species	Frequency (cm^{-1})			Relative energy (kcal mol^{-1})
Scan Point-1	72.0472	85.3668	119.6913	
	141.8873	172.182	198.6829	
	528.6092	691.8923	753.3696	
	882.1323	896.0601	1025.7254	-9.64
	1091.183	1259.1944	1446.3351	
	1486.6322	1671.6883	1801.2655	
	3139.8607	3285.9742	3373.2087	
Scan Point-2	53.8438	68.17	95.4146	
	104.4047	131.4761	170.3893	
	531.1474	695.172	740.8156	
	799.1109	893.3451	1001.2602	
	1081.609	1259.3736	1435.0836	-8.36
	1443.3452	1663.5454	1806.7149	
	3137.8985	3285.4217	3592.4762	
Scan Point-3	-90.6331	6.2395	37.7901	
	57.4614	86.551	118.4394	
	534.5561	680.5962	695.5148	
	724.7735	907.7885	961.167	
	1055.5674	1260.4763	1376.6954	-4.58
	1439.1319	1650.9007	1817.106	
	3137.4678	3286.7874	3755.7487	
Scan Point-4	-69.7695	5.3935	10.9458	
	43.9515	64.1281	81.3747	
	536.1642	633.0978	694.9538	
	717.6146	914.5339	938.3456	
	1043.6448	1260.5429	1361.068	-1.93
	1437.2486	1643.7864	1825.5422	
	3138.0982	3287.7498	3800.4259	
Scan Point-5	-27.8842	5.4155	12.423	
	19.4403	28.4087	43.3386	
	538.5971	597.2355	696.645	
	705.9114	912.9463	926.5926	-0.31
	1028.0999	1261.9007	1345.8657	
	1435.0396	1632.8251	1836.2296	
	3139.3295	3289.9169	3822.842	
Scan Point-6	-21.0586	5.3307	6.3071	
	10.9094	19.8618	33.2546	
	539.1014	588.8627	699.2447	
	703.2559	908.3438	928.2325	
	1026.2229	1262.3693	1344.1959	-0.09
	1434.9608	1631.1099	1839.1739	
	3139.8202	3290.1398	3826.2428	
Scan Point-7	-44.4326	5.2855	7.1627	
	10.3705	14.9963	27.4379	
	538.6783	567.1913	698.2217	-0.01
	701.2316	905.9958	928.5185	
	1024.6854	1261.1973	1341.0072	
	1434.17	1630.9416	1839.505	
	3139.5169	3290.9253	3835.6673	

S2 Details of the methodology used for the electronic structure theory

To estimate energies at CCSD(T)/CBS level of theory, first we calculated the single point energies at CCSD(T)/aug-cc-pVDZ, and CCSD(T)/aug-cc-pVTZ level of theory, and then extrapolated these energies to corresponding CBS limit using the method of Varandas and Pansini.[2,3] Specifically, for the extrapolation of correlation energies, the following equation is used:

$$\mathrm{CBS(Corr)} = \frac{2.71^3\mathrm{E_{ATZ}} - 1.91^3\mathrm{E_{ADZ}}}{2.71^3 - 1.91^3}$$

Where, E_{ADZ} and E_{ATZ} are correlation energies at CCSD(T)/aug-cc-pVDZ and CCSD(T)/aug-cc-pVTZ level of theory, respectively. For the extrapolation of Hartree-Fock energies, the following equation is used:

$$\mathrm{CBS(HF)} = \frac{2.96^5\mathrm{E_{ATZ}} - 2.08^5\mathrm{E_{ADZ}}}{2.96^5 - 2.08^5}$$

Where, E_{ADZ} and E_{ATZ} are Hartree-Fock energies at CCSD(T)/aug-cc-pVDZ and CCSD(T)/aug-cc-pVTZ level of theory, respectively.

Table S4: Different components of post-CCSD(T) corrections for CH_2OO + HONO reaction. All energetic values are in kcal mol^{-1}.

Species	**CCSD(T)/CBS**	**T**	**T(Q)**	**ZPE**	**Final**
RC1	-11.59	0.05	0.49	1.45	-9.59
TS1	-9.02	0.12	0.55	1.03	-7.31

S3 Details of kinetic modelling

The kinetic model has been developed using a Reaction system module from chempy.[4] This model requires two key components: first, a list of relevant reactions along with their rate coefficients, and second, a list of realistic initial concentrations of the reactive species in-

volved in the reactions. In principle, we solve a system of ordinary differential equations (ODEs) that describe the time-dependent changes in the concentrations of $OH^{\bullet}$ and $HO_2^{\bullet}$. We have performed this kinetic modeling at room temperature. The system is simulated for 60 minutes using a high-resolution time grid with 50,000 time steps to capture rapid chemical kinetics. Stringent absolute (atol=1e-8) and relative (rtol=1e-8) tolerances are applied to maintain numerical stability and precision. We first tracked the change in concentration of $OH^{\bullet}$ and $HO_2^{\bullet}$ using kinetic model consisting of CH_2OO + HONO reaction (M-1), followed by the second model consisting of $(CH_3)_2COO$ + HONO reaction (M-2). The reaction mechanism included three bimolecular reactions which can be initiated from the title reaction as mentioned in the box (main manuscript). Initial concentrations of relevant species (HCHO, $(CH_3)_2CO$, and $HO_2^{\bullet}$) were chosen based on literature values representing polluted urban conditions.[5] Although the average concentration of NO_2, and $OH^{\bullet}$ are found to be $\sim 10^6$ and $\sim 10^{12}$ molecules cm^{-3} in the atmosphere, we have used modelled value of them in the present work. In CH_2OO + HONO reaction model, the initial OH radical concentration was set to $\sim 10^4$ molecules cm^{-3}, while in $(CH_3)_2COO$ + HONO model, it was set to $\sim 10^5$ molecules cm^{-3}. Similarly, the concentration of NO_2 was kept to be $\sim 10^{10}$ molecules cm^{-3} for both the kinetic modelling in order to observe a clear numerical change in the values of $HO_2^{\bullet}$.

Table S5: List of all reactions and their corresponding rate coefficients, along with the model concentrations of the relevant species at 298 K.

Reactions	$\mathbf{k_{298}}$	**Species**	**Concentration**
$CH_2OO + HONO \rightarrow HCHO + NO_2 + OH$	7.21×10^{-12}	CH_2OO/C_2H_6COO[6]	1.00×10^{5}
$C_2H_6COO + HONO \rightarrow C_2H_6CO + NO_2 + OH$	2.03×10^{-11}	$HCHO/C_2H_6O$[5]	5.10×10^{11}
$HCHO + HO_2 \rightarrow HOCH_2OO$[7]	6.27×10^{-14}	HONO[8]	8.90×10^{10}
$C_2H_6CO + HO_2 \rightarrow HOC_2H_6COO$[9]	4.40×10^{-13}	NO_2 (M-1/M-2)	1.00×10^{10}
$NO_2 + HO_2 \rightarrow HNO_4$[10]	5.40×10^{-12}	OH(M-1)	2.30×10^{4}
		OH(M-2)	2.30×10^{5}
		HO_2[5]	7.00×10^{8}

S4 Gibbs free energy

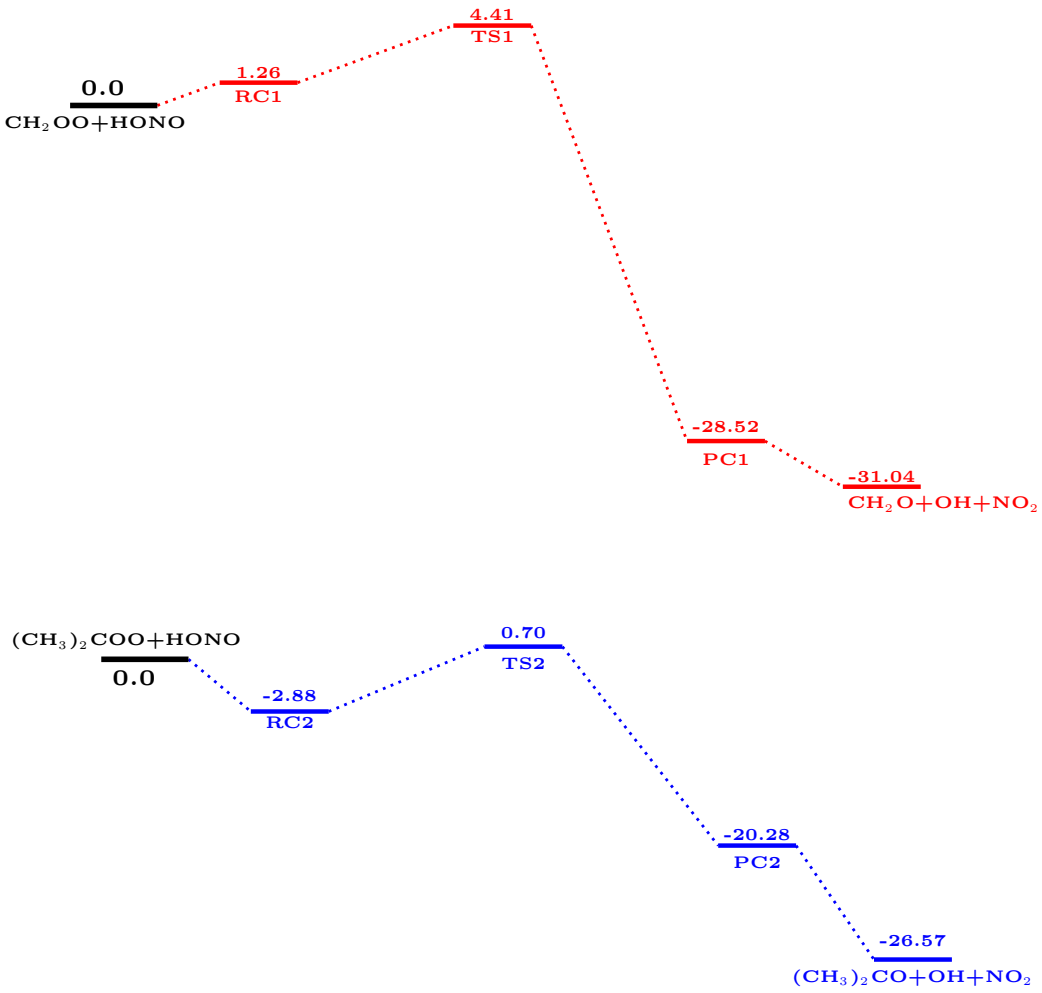

Figure S2: Top panel: Gibbs free energy profile (kcal mol^{-1}) for CH_2OO + HONO reaction obtained at CCSD(T)/CBS level of theory at 298 K. Bottom panel: Gibbs free energy profile (kcal mol^{-1}) for $(CH_3)_2COO$ + HONO reaction obtained at same level of theory at 298 K.

S5 Relevant rate constants

Table S6: The capture rate for both, CH_2OO + HONO and $(CH_3)_2COO$ + HONO reaction.

Temp.	k_f	$k_f^{'}$
213	1.46×10^{-10}	1.20×10^{-10}
216	1.49×10^{-10}	1.21×10^{-10}
219	1.51×10^{-10}	1.22×10^{-10}
224	1.56×10^{-10}	1.24×10^{-10}
235	1.65×10^{-10}	1.28×10^{-10}
250	1.77×10^{-10}	1.33×10^{-10}
259	1.84×10^{-10}	1.36×10^{-10}
265	1.88×10^{-10}	1.38×10^{-10}
278	1.97×10^{-10}	1.42×10^{-10}
280	1.99×10^{-10}	1.43×10^{-10}
290	2.05×10^{-10}	1.45×10^{-10}
298	2.09×10^{-10}	1.47×10^{-10}
300	2.10×10^{-10}	1.47×10^{-10}
310	2.15×10^{-10}	1.49×10^{-10}
320	2.20×10^{-10}	1.51×10^{-10}

Table S7: The bimolecular rate constant, average concentration in the polluted environment and effective rate constant for CH_2OO + X (where X = SO_2, NO_2, NO, CO, H_2O, and $(H_2O)_2$).

Reaction	k_{bi}^{298K}	[X] (molecule cm^{-3})	k_{eff} (sec^{-1})
$CH_2OO + SO_2$ [5,11]	3.72×10^{-11}	9.00×10^{10}	3.35
$CH_2OO + NO_2$ [5,12]	1.00×10^{-12}	9.00×10^{11}	0.90
$CH_2OO + NO$ [5,13]	$< 6.00\times10^{-14}$	9.00×10^{10}	0.01
$CH_2OO + CO$ [5,14]	$< 2.0\times10^{-16}$	3.00×10^{13}	0.01
$CH_2OO + H_2O$ *(RH=20%)* [15–17]	3.13×10^{-16}	1.53×10^{17}	47.73
$CH_2OO + (H_2O)_2$ *(RH=20%)* [15–17]	5.48×10^{-12}	4.76×10^{13}	260.96
$CH_2OO + H_2O$ *(RH=100%)* [15–17]	3.13×10^{-16}	7.63×10^{17}	238.64
$CH_2OO + (H_2O)_2$ *(RH=100%)* [15–17]	5.48×10^{-12}	1.19×10^{15}	6524.00

Table S8: Comparison between the unimolecular rate of $(CH_3)_2COO$ [18] and effective rate constant of $(CH_3)_2COO$ + HONO reaction.

Temp.	k_{uni} (s^{-1}) [18]	k_{eff} (s^{-1})
213	1.82	3.80
216	2.18	3.71
219	2.60	3.64
224	3.49	3.50
235	6.73	3.21
250	16.47	2.83
259	28.12	2.61
265	40.13	2.47
278	86.25	2.19
280	96.95	2.15
290	173.46	1.95
298	275.08	1.80
300	308.50	1.77
310	545.19	1.60
320	956.98	1.44

Table S9: The capture rate and bimolecular rate constant for CH_2OO + HONO reaction at post-CCSD(T) level.

Temp.	k_f	$k_{bi}^{CH_2OO}$
213	9.05×10^{-11}	1.11×10^{-11}
216	9.17×10^{-11}	1.08×10^{-11}
219	9.30×10^{-11}	1.06×10^{-11}
224	9.51×10^{-11}	1.01×10^{-11}
235	9.95×10^{-11}	9.24×10^{-12}
250	1.05×10^{-10}	8.17×10^{-12}
259	1.08×10^{-10}	7.59×10^{-12}
265	1.11×10^{-10}	7.22×10^{-12}
278	1.15×10^{-10}	6.50×10^{-12}
280	1.15×10^{-10}	6.40×10^{-12}
290	1.19×10^{-10}	5.90×10^{-12}
298	1.21×10^{-10}	5.53×10^{-12}
300	1.21×10^{-10}	5.44×10^{-12}
310	1.24×10^{-10}	5.03×10^{-12}
320	1.26×10^{-10}	4.64×10^{-12}

Table S10: The capture rate for dissociation of PC1 and PC2 to corresponding isolated products.

Temp.	k_{PC1}	k_{PC2}
213	1.79×10^{12}	1.32×10^{12}
216	1.79×10^{12}	1.33×10^{12}
219	1.80×10^{12}	1.33×10^{12}
224	1.81×10^{12}	1.34×10^{12}
235	1.83×10^{12}	1.35×10^{12}
250	1.85×10^{12}	1.36×10^{12}
259	1.86×10^{12}	1.36×10^{12}
265	1.87×10^{12}	1.37×10^{12}
278	1.89×10^{12}	1.38×10^{12}
280	1.89×10^{12}	1.38×10^{12}
290	1.90×10^{12}	1.39×10^{12}
298	1.91×10^{12}	1.39×10^{12}
300	1.91×10^{12}	1.39×10^{12}
310	1.93×10^{12}	1.40×10^{12}
320	1.94×10^{12}	1.40×10^{12}

References

(1) Johnson III, R. D. NIST computational chemistry comparison and benchmark database, NIST standard reference database number 101. *Release 16a http://cccbdb.nist.gov/ (accessed march 5, 2025)* **2013**,

(2) Varandas, A.; Pansini, F. Narrowing the error in electron correlation calculations by basis set re-hierarchization and use of the unified singlet and triplet electron-pair extrapolation scheme: Application to a test set of 106 systems. *J. Chem. Phys.* **2014**, *141*, 224113.

(3) Pansini, F.; Neto, A.; Varandas, A. Extrapolation of Hartree–Fock and multiconfiguration self-consistent-field energies to the complete basis set limit. *Theor. Chem. Acc.* **2016**, *135*, 1–6.

(4) Dahlgren, B. ChemPy: A package useful for chemistry written in Python. *J. Open Source Softw.* **2018**, *3*, 565.

(5) Vereecken, L.; Harder, H.; Novelli, A. The reaction of Criegee intermediates with NO, RO_2, and SO_2, and their fate in the atmosphere. *Phys. Chem. Chem. Phys.* **2012**, *14*, 14682–14695.

(6) Khan, M.; Percival, C.; Caravan, R.; Taatjes, C.; Shallcross, D. Criegee intermediates and their impacts on the troposphere. *Environ. Sci.: Process. Impacts* **2018**, *20*, 437–453.

(7) Gao, Q.; Shen, C.; Zhang, H.; Long, B.; Truhlar, D. G. Quantitative kinetics reveal that reactions of HO_2 are a significant sink for aldehydes in the atmosphere and may initiate the formation of highly oxygenated molecules via autoxidation. *Phys. Chem. Chem. Phys.* **2024**, *26*, 16160–16174.

(8) Pawar, P. V.; Mahajan, A. S.; Ghude, S. D. HONO chemistry and its impact on the atmospheric oxidizing capacity over the Indo-Gangetic Plain. *Sci. Total Environ.* **2024**, 174604.

(9) Hermans, I.; Nguyen, T. L.; Jacobs, P. A.; Peeters, J. Tropopause chemistry revisited: $HO_2^{\bullet}$-initiated oxidation as an efficient acetone sink. *J. Am. Chem. Soc.* **2004**, *126*, 9908–9909.

(10) Christensen, L. E.; Okumura, M.; Sander, S. P.; Friedl, R. R.; Miller, C. E.; Sloan, J. J. Measurements of the Rate Constant of $HO_2 + NO_2 + N_2 \longrightarrow HO_2NO_2 + N_2$ Using Near-Infrared Wavelength-Modulation Spectroscopy and UV- Visible Absorption Spectroscopy. *J. Phys. Chem. A* **2004**, *108*, 80–91.

(11) Onel, L.; Lade, R.; Mortiboy, J.; Blitz, M. A.; Seakins, P. W.; Heard, D. E.; Stone, D. Kinetics of the gas phase reaction of the Criegee intermediate CH_2OO with SO_2 as a function of temperature. *Phys. Chem. Chem. Phys.* **2021**, *23*, 19415–19423.

(12) Luo, P.-L.; Chung, C.-A.; Lee, Y.-P. Rate coefficient of the reaction $CH_2OO+ NO_2$ probed with a quantum-cascade laser near 11 μm. *Phys. Chem. Chem. Phys.* **2019**, *21*, 17578–17583.

(13) Cox, R. A.; Ammann, M.; Crowley, J. N.; Herrmann, H.; Jenkin, M. E.; McNeill, V. F.; Mellouki, A.; Troe, J.; Wallington, T. J. Evaluated kinetic and photochemical data for atmospheric chemistry: Volume VII–Criegee intermediates. *Atmos. Chem. Phys.* **2020**, *20*, 13497–13519.

(14) Eskola, A. J.; Döntgen, M.; Rotavera, B.; Caravan, R. L.; Welz, O.; Savee, J. D.; Osborn, D. L.; Shallcross, D. E.; Percival, C. J.; Taatjes, C. A. Direct kinetics study of CH_2OO+ methyl vinyl ketone and CH_2OO+ methacrolein reactions and an upper limit determination for CH_2OO+ CO reaction. *Phys. Chem. Chem. Phys.* **2018**, *20*, 19373–19381.

(15) Lin, L.-C.; Chang, H.-T.; Chang, C.-H.; Chao, W.; Smith, M. C.; Chang, C.-H.; Lin, J. J.-M.; Takahashi, K. Competition between H_2O and $(H_2O)_2$ reactions with CH_2OO/CH_3CHOO. *Phys. Chem. Chem. Phys.* **2016**, *18*, 4557–4568.

(16) Anglada, J. M.; Hoffman, G. J.; Slipchenko, L. V.; M. Costa, M.; Ruiz-Lopez, M. F.; Francisco, J. S. Atmospheric significance of water clusters and ozone–water complexes. *J. Phys. Chem. A* **2013**, *117*, 10381–10396.

(17) Rai, P. K.; Kumar, P. Influence of Water on the NO_3 + HO_2 Reaction. *J. Phys. Chem. A* **2025**, *129*, 2067–2076.

(18) Fang, Y.; Barber, V. P.; Klippenstein, S. J.; McCoy, A. B.; Lester, M. I. Tunneling Effects in the Unimolecular Decay of $(CH_3)_2COO$ Criegee Intermediates to OH Radical Products. *J. Chem. Phys.* **2017**, *146*, 134307.